

AD-A109 906

HARVARD UNIV CAMBRIDGE MA DIV OF APPLIED SCIENCES

F/8 11/2

EFFECT OF QUENCH RATE ON THE STRUCTURAL RELAXATION OF A METALLI--ETC(U)

JAN 62 A L GREER

N00014-77-C-0002

ML

UNCLASSIFIED

TR-12

For
AD
DATA



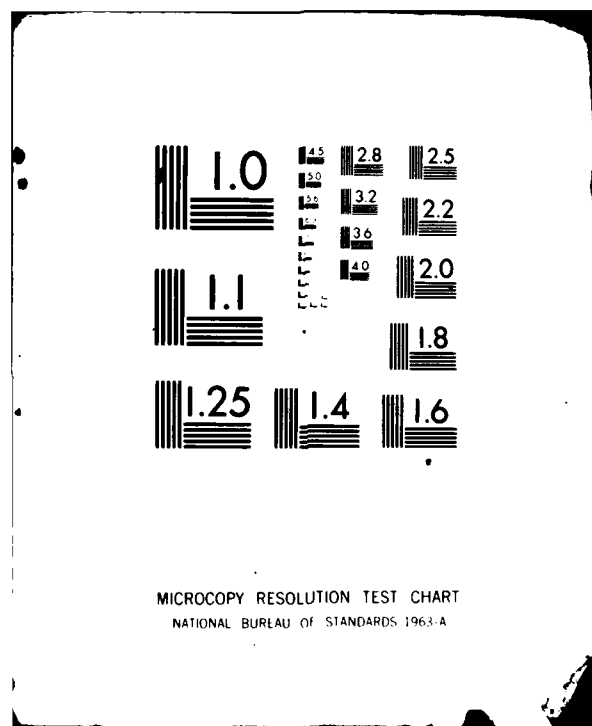
END

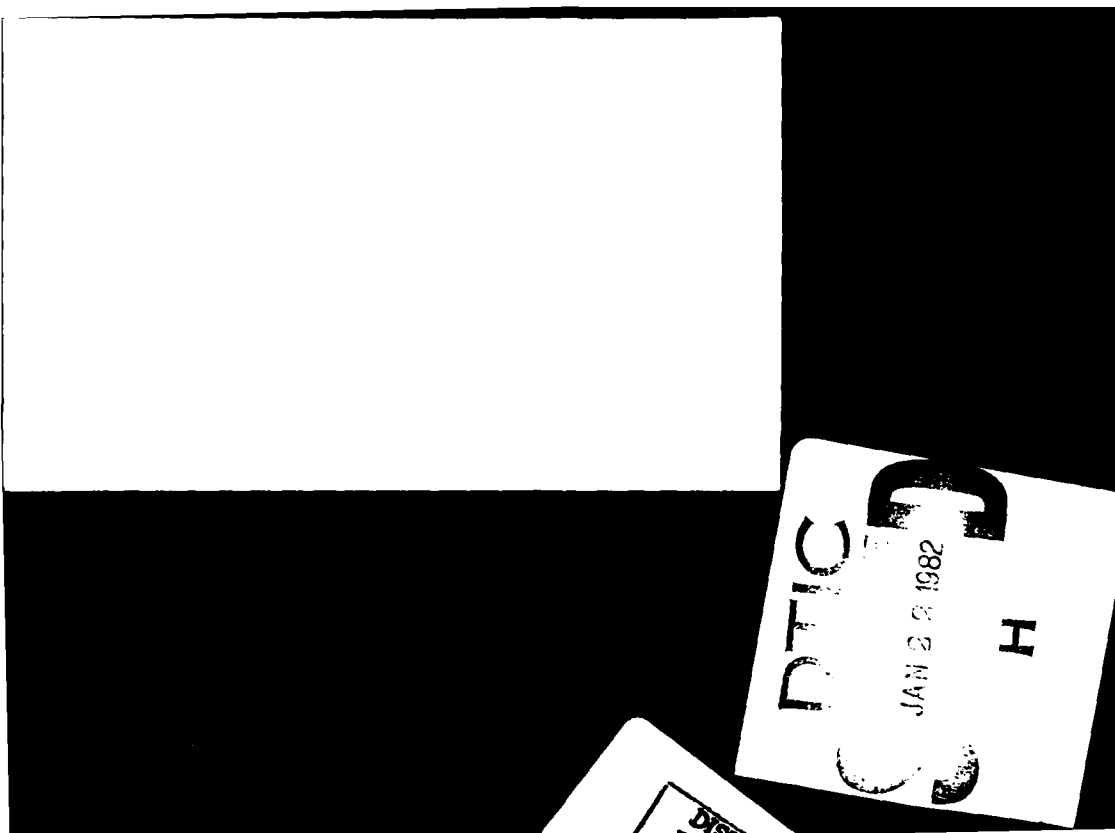
DATE

FILED

3-82

DTIC





Office of Naval Research

Contract N00014-77-C-0002 NR-039-136

EFFECT OF QUENCH RATE ON THE STRUCTURAL
RELAXATION OF A METALLIC GLASS

by

A.L. Greer

DTIC
SELECTED
JAN 22 1982
D
H

Technical Report No. 12

This document has been approved for public release and sale; its distribution is unlimited. Reproduction in whole or in part is permitted by the U. S. Government.

January 1982

The research reported in this document was made possible through support extended the Division of Applied Sciences, Harvard University, by the Office of Naval Research, under Contract N00014-77-C-0002.

Division of Applied Sciences

Harvard University • Cambridge, Massachusetts

Unclassified

SECURITY CLASSIFICATION OF THIS PAGE (When Data Entered)

REPORT DOCUMENTATION PAGE		READ INSTRUCTIONS BEFORE COMPLETING FORM
1. REPORT NUMBER Technical Report No. 12	2. GOVT ACCESSION NO. AD A109906	3. RECIPIENT'S CATALOG NUMBER TI-12
4. TITLE (and Subtitle) EFFECT OF QUENCH RATE ON THE STRUCTURAL RELAXATION OF A METALLIC GLASS		5. TYPE OF REPORT & PERIOD COVERED Interim Report
		6. PERFORMING ORG. REPORT NUMBER
7. AUTHOR(s) A.L. Greer		8. CONTRACT OR GRANT NUMBER(s) N00014-77-C-0002
9. PERFORMING ORGANIZATION NAME AND ADDRESS Division of Applied Sciences Harvard University Cambridge, MA 02138		10. PROGRAM ELEMENT, PROJECT, TASK AREA & WORK UNIT NUMBERS
11. CONTROLLING OFFICE NAME AND ADDRESS		12. REPORT DATE January 1982
		13. NUMBER OF PAGES 30
14. MONITORING AGENCY NAME & ADDRESS (if different from Controlling Office)		15. SECURITY CLASS. (of this report) Unclassified
		16a. DECLASSIFICATION/DOWNGRADING SCHEDULE
16. DISTRIBUTION STATEMENT (of this Report) This document has been approved for public release and sale; its distribution is unlimited. Reproduction in whole or in part is permitted by the U.S. Government.		
17. DISTRIBUTION STATEMENT (of the abstract entered in Block 20, if different from Report)		
18. SUPPLEMENTARY NOTES		
19. KEY WORDS (Continue on reverse side if necessary and identify by block number) Metallic glasses Quench rate Structural Relaxation Curie temperature Magnetic properties		
20. ABSTRACT (Continue on reverse side if necessary and identify by block number) Measurements of the ferromagnetic Curie temperature, T_c , have been used to monitor the structural relaxation of the metallic glass $Fe_{81.5}B_{14.5}Si_4$. The glass was produced by melt-spinning to various ribbon thicknesses at consequently different quench rates. It is shown that faster quenched (i.e. thinner) ribbons have lower initial T_c 's, corresponding to less relaxed structures. All the materials,		

DD FORM 1 JAN 73 1473

EDITION OF 1 NOV 65 IS OBSOLETE
S/N 0102-014-6601

Unclassified

SECURITY CLASSIFICATION OF THIS PAGE (When Data Entered)

Unclassified

SECURITY CLASSIFICATION OF THIS PAGE(When Data Entered)

however, tend to the same equilibrium on annealing. An effect which is particularly marked at low annealing temperatures is that faster quenched ribbons relax faster. The results are interpreted in terms of two relaxation mechanisms.

of

Unclassified

SECURITY CLASSIFICATION OF THIS PAGE(When Data Entered)

EFFECT OF QUENCH RATE ON THE STRUCTURAL RELAXATION OF A METALLIC GLASS

A.L. Greer

Division of Applied Sciences
Harvard University, Cambridge, MA 02138, USA

SYNOPSIS

Measurements of the ferromagnetic Curie temperature, T_c , have been used to monitor the structural relaxation of the metallic glass $\text{Fe}_{81.5}\text{B}_{14.5}\text{Si}_4$. The glass was produced by melt-spinning to various ribbon thicknesses at consequently different quench rates. It is shown that faster quenched (i.e. thinner) ribbons have lower initial T_c 's, corresponding to less relaxed structures. All the materials, however, tend to the same equilibrium on annealing. An effect which is particularly marked at low annealing temperatures is that faster quenched ribbons relax faster. The results are interpreted in terms of two relaxation mechanisms.

Accession For	
NTIS	<input checked="" type="checkbox"/>
DTIC	<input type="checkbox"/>
Unannounced	<input type="checkbox"/>
Justification	<input type="checkbox"/>
By _____	
Distribution _____	
Availability Codes _____	
or _____	
DTIC _____	
A	

DTIC
COPY
INSPECTED
3

EFFECT OF QUENCH RATE ON THE STRUCTURAL RELAXATION OF A METALLIC GLASS

A.L. Greer

Division of Applied Sciences
Harvard University, Cambridge, MA 02138 USA

1. INTRODUCTION

Annealing metallic glasses causes substantial property changes. It is reasonable to suppose that changes in production conditions would give rise to property variations of similar magnitude. Indeed, some of the discrepancies between results from different workers may indicate such effects. It is important to understand the effects of production variables, not only for optimisation of the production, but also in more fundamental studies of metallic glasses. For example, if the property variations arising from the production were similar to those due to composition changes, the interpretation of the effects of composition would be greatly hampered.

Considering their importance, there have been rather few studies of the effects of production variables. This is in large part due to the difficulty of varying the parameters in a controlled way, while still obtaining a glassy product. Metallic glasses can be produced in many ways, but in this paper only those made by melt-spinning [1] will be considered. In melt-spinning there are many parameters which can be adjusted, including the melt superheat and the flow in the molten alloy jet. One of the most controlled experiments, however, is to vary the wheel speed while keeping all other parameters fixed. Experimentally [2,3] the ribbon thickness, D , appears to vary with the wheel speed, V as:

$$D \propto V^{-a} \text{ where } a \approx 0.75 \quad (1)$$

Thus higher wheel speed gives a thinner ribbon, but the width is only slightly affected. It is expected that a thinner ribbon will have been quenched at a higher average rate, R [4]:

$$R \propto D^{-1} \text{ for Newtonian cooling} \quad (2)$$

$$R \propto D^{-2} \text{ for ideal cooling} \quad (3)$$

It seems that Newtonian cooling is more likely, i.e. that heat transfer across the ribbon-substrate interface is rate-controlling. The quench rate will vary during the cooling from the melt to the final ribbon, but it is desirable to characterise the production by an average quench rate R . The ribbon thickness, D , a readily measured quantity, at least gives the order of R in a series of samples, and may be used to estimate relative values.

The property changes on annealing metallic glasses may be due to: the relief of quenched-in internal stresses, which occurs early in the anneal; the structural relaxation of the glassy state; or, in the later stages of the anneal, the onset of crystallisation or of separation into two glassy phases. The effects of quench rate are expected to be analogous, i.e. the property differences between slow-quenched and fast-quenched glasses should be similar to the differences between annealed and unannealed glasses. For example, higher rates appear to quench in higher internal stresses [5]. Also, at low rates a partially crystalline product may be obtained. The third effect is on the degree of relaxation of the glassy structure. A metallic glass, in common with other glasses, does not have a unique structural state. A more slowly quenched glass will have a more

relaxed structure, akin to what would be obtained on annealing a faster quenched glass. In this paper the concern will be with the effect of quench rate on the degree of relaxation of the as-produced glass and on the kinetics of the subsequent relaxation induced by annealing. From the published studies [6-16] of the effect of production variables on the properties of metallic glasses, the work which seems relevant in the present case is summarised below.

For metallic glass ribbons the rate of relaxation of an externally applied stress can be measured readily [17]. The relaxation on annealing is rapid at first, then slower. Williams and Egami [18] have shown that pre-annealing greatly reduces the stress relaxation rate. These observations support the view that an annealed, i.e. more structurally relaxed, glass will have lower atomic mobility. Luborsky and Walter [10] showed that thinner, i.e. faster quenched, ribbons exhibited faster stress relaxation. Their results have been amply confirmed [8, 11, 15] and constitute perhaps the clearest evidence so far of the effect of quench rate on the degree of structural relaxation of metallic glasses.

Allia *et al.* [16] have measured the relative decay of magnetic permeability on annealing. This process also is faster in more rapidly quenched ribbons. The differences in behaviour due to the quench rate are reduced by pre-annealing.

Metallic glasses embrittle on annealing. One would expect that the rate of embrittlement would be greater in faster quenched ribbons. In contrast, however, it is found that faster quenched ribbons embrittle less easily [8,15], i.e. after longer times or at higher temperatures. This effect can be explained if it is assumed that embrittlement corresponds to a critical degree of structural relaxation. Faster quenched glasses may

indeed relax faster, but their starting condition is further from the critical relaxation, and they may therefore take longer to attain it.

The main technological interest in metallic glasses is because of their magnetic properties. These properties are particularly sensitive to annealing and to quench rate, but are not easily interpreted in terms of structural relaxation. The coercivity, for example, is probably more strongly affected by internal stresses and incipient crystallisation than by relaxation. The Curie temperature, T_c , however, is a useful parameter for studying structural relaxation, being sensitive to the relaxation and convenient to measure [19]. It is unaffected by relief of internal stresses and often unaffected by partial crystallisation [20]. The disadvantages of using T_c are that it cannot be monitored continuously, and that if T_c is too high, unavoidable relaxation may occur during the determination, thereby obscuring any effects of pre-annealing. The Curie temperature of metallic glasses rises on annealing. It is therefore expected that faster quenched glasses will have lower T_c . Mizoguchi *et al.* [12] have confirmed this. A negative result by Takayama and Oi [9] was due to the relaxation during the T_c determinations, because of the high T_c of their alloy.

An important feature of the T_c studies of relaxation is that at higher annealing temperatures the T_c eventually levels off after rising rapidly at first. The attainment of a final value of T_c signifies that an "internal equilibrium" has been reached. This may be true internal equilibrium, when the configuration of the metastable liquid is realised, or it may be a "local equilibrium" constrained by some slow relaxations. It has been suggested [21] that the former case applies to $Fe_{80}B_{20}$ and the latter to more complex glasses. In either case the behaviour is as

for true equilibrium, since the final values of T_c appear to be functions of temperature only and can be approached from higher or lower values.

In the light of this, and of the embrittlement results mentioned above, the present aim is to use T_c measurements to answer two questions:

- (1) Given that different degrees of relaxation can be obtained by quenching at different rates, will the various glasses relax to the same "equilibrium" structure on annealing?
- (2) if so, will a fast-quenched or a slow-quenched glass attain "equilibrium" sooner?

2. EXPERIMENTAL PROCEDURE

$\text{Fe}_{81.5}\text{B}_{14.5}\text{Si}_4$ ribbons (composition in atomic %) were kindly supplied by Drs. H.H. Liebermann and F.E. Luborsky of the General Electric Company. The ribbons, in five thicknesses, had been produced as part of a study of the effect of process variables on the properties of amorphous alloys [15]. They were prepared by melt-spinning on a 25 cm diameter wheel. The wheel speed was varied while all other parameters were held constant. The thickness of the ribbons, which was approximately inversely proportional to the wheel speed, varied from 16.0 μm to 58.2 μm .

The Curie temperatures were determined by differential scanning calorimetry using a Perkin Elmer DSC 2. A heating rate of 80 K min^{-1} was used. General aspects of the technique are described elsewhere [19]. The T_c values were corrected for the temperature lag in the instrument by measuring them relative to the T_c of a nickel standard placed in the sample pan for each determination. Only one T_c determination was carried out on a given DSC sample. It was necessary to run up to six samples to obtain the T_c value, because there was some scatter.

Annealing was carried out in the differential scanning calorimeter. this has excellent temperature control (± 0.1 K) and was calibrated to ± 0.5 K. The DSC was also used for crystallisation studies; in this case the samples were heated at 40 K min^{-1} . Transmission electron microscopy was performed in a JEM 120 instrument operated at 80 KV. Thin foils were prepared by ion milling pre-annealed ribbons.

3. RESULTS AND DISCUSSION

3.1 General relaxation behaviour

It was necessary first to verify that the structural relaxation behaviour of $\text{Fe}_{81.5}\text{B}_{14.5}\text{Si}_4$ glass was similar to that of other iron-based metallic glasses, and that it could be monitored by measuring the Curie temperature. Figure 1 shows that the measured T_C of a ribbon of $\text{Fe}_{81.5}\text{B}_{14.5}\text{Si}_4$ glass varies strongly with the heating rate used to determine T_C . This is a real variation and does not arise from the temperature lags in the instrument which have been accounted for. T_C is higher at slower heating rates, because of the greater annealing effect during the determination. Such effects are undesirable (reflecting a rather high T_C in this case), but can be minimised by using high heating rates (80 K min^{-1} in the present work). Fortunately the annealing effect during the determinations is not sufficient to obscure the effects of pre-annealing. The data on Figure 1 indicate that annealing causes the T_C of $\text{Fe}_{81.5}\text{B}_{14.5}\text{Si}_4$ glass to rise, in common with other iron-based glasses. In general, annealing these glasses at any temperature causes T_C to rise rapidly at first and then level off. The higher the annealing temperature, the more rapid is the T_C rise, but the lower the final value of T_C [21]. A common way of observing this behaviour is through a series of isochronal anneals. Figure 2 shows the results of this experiment on two ribbons of $\text{Fe}_{81.5}\text{B}_{14.5}\text{Si}_4$ glass. The change in Curie temperature ΔT_C is plotted against the annealing temperature, T_a , for 15-minute anneals. The expected result is a peak in ΔT_C : at high temperatures, above the peak, the glass gets close to "equilibrium" in the time of the anneal, and the slope of the curve reflects the variation of final T_C with T_a ; at lower temperatures, however, the glass is still far from "equilibrium",

and the shape of the curve illustrates the faster kinetics as T_a is raised. It can be seen from Figure 2 that here is a peak in ΔT_c at about 630 K, but this is followed by a sharp rise. It has been suggested that such a rise in other systems could be due to the onset of crystallisation [20], and for the present case that will be verified in the next section. The conclusion of this section is that the structural relaxation of $\text{Fe}_{81.5}\text{B}_{14.5}\text{Si}_4$ glass, as revealed by T_c changes, is similar to that of iron-based glasses in general. The two curves in Figure 2 give the first indication of the effect of ribbon thickness, i.e. quench rate, on relaxation behaviour, which is the main concern of this paper.

3.2 Crystallisation

Samples of all the ribbons of the glass were heated at 40 K min^{-1} in the differential scanning calorimeter. In all cases two peaks were found on the trace, as illustrated in Figure 3 for the $21.6 \mu\text{m}$ thick ribbon. The two peaks indicate two reactions. It was found that pre-annealing could be used to drive the first reaction to completion. For example, an anneal at 719 K for 20 minutes has this effect (Figure 3). After this anneal the microstructure was examined by transmission electron microscopy. This shows that the first reaction ("primary crystallisation") consists of the precipitation of $\alpha\text{-Fe}$ in a highly dendritic form (Figure 4). The dendrite arms are parallel to $[100] \alpha\text{-Fe}$. Some of the crystals appear to be twinned. As far as it is possible to assess, the orientation of the crystals appears to be random. The crystallisation morphology is remarkably similar to that found by Swartz *et al.* in a $\text{Fe}_{81}\text{B}_{13.5}\text{Si}_{3.5}\text{C}_2$ glass [22,23].

The effect of partial crystallisation on the Curie temperature of

the remaining amorphous phase was studied on annealing at 718 K. The rise in T_c is shown in Figure 5, and at each stage the percentage total primary crystallisation is indicated. This percentage was estimated from the relative decrease in the area of the first DSC peak. At this comparatively high annealing temperature it is expected that any rise in T_c due to structural relaxation will be over quickly ($\ll 5$ min.), so that the continuing rise at longer times is due to the changing composition of the remaining amorphous phase as the growing α -Fe crystals reject B and Si into it. Such a rise is consistent with the results of Durand and Yung [24] who have shown that the T_c of iron-based glasses rises as the metalloid (particularly B) content is increased. After 15 minutes at 718 K the T_c of the amorphous matrix was not detectable by DSC. It is not clear why this is so, but it may be because the magnetic transition is blurred by substantial composition gradients in the matrix. It is concluded that in this alloy primary crystallisation of α -Fe causes the T_c of the remaining amorphous phase to rise, and that the rise in ΔT_c above 650 K in Figure 2 can reasonably be attributed to this. By annealing at lower temperatures this effect can be avoided, and the T_c changes can be attributed to structural relaxation alone.

The DSC curves for the as-received ribbons (e.g. for the 21.6 μm ribbon in Figure 3) were all identical except for the thickest ribbon (58.2 μm), for which the first peak occurred about 1 K lower. This would be consistent with a small degree of crystallinity [25]. The magnetic properties determined by Luborsky *et al.*, [15] suggest that not only this sample, but also the next thickest (41.7 μm) could be slightly crystalline.

3.3 Effect of quench rate

The Curie temperatures of the as-quenched ribbons are shown as a function of thickness in Figure 6. Each point represents the average of six determinations and the standard error is shown. As expected, T_c is lower for the thinner, i.e. faster quenched, ribbons. The thinnest ribbon, however, appears to be anomalous.

It is known that there is an annealing effect during the T_c determination (Figure 1). If that effect were greater for the 16.0 μm ribbon it could explain its high value of T_c . In fact, though, this ribbon exhibited the same variation of T_c with heating rate as in Figure 1. Its anomalously high value of T_c in the as-quenched state is a real effect.

Partial crystallinity of the 41.7 μm and 58.2 μm ribbons could make a small contribution to their high T_c values. In any case, measurements on them show a wider scatter than for the other samples.

Figure 7 shows the effect of annealing the ribbons at 633 K. In all the ribbons T_c rises rapidly at first and then begins to level off at a final "equilibrium" value. It appears that all the glasses are tending to the same equilibrium - compare the spread in initial T_c values with the spread after 360 minutes of anneal. It is also noteworthy that the curves in Figure 7 do not cross: although at any instant the faster quenched ribbons (with lower initial T_c) do relax faster, their T_c values do not "overtake" those of the more slowly quenched ribbons. Thus to reach "equilibrium", or any given value of T_c it will take a faster quenched glass longer, despite its greater atomic mobility. This is precisely the effect needed to explain the embrittlement results in the Introduction. The 16.0 μm and 25.8 μm ribbons not only have similar initial T_c 's, but their behaviour on annealing at 633 K is almost identical.

This leads to the speculation that these ribbons, despite their different thicknesses, might somehow have been quenched at the same rate.

The relaxation behaviour is very different on annealing at a lower temperature, 573 K. In this case, shown in Figure 8, the faster quenched glasses relax so much faster that the T_c curves do cross. At 573 K "equilibrium" is not reached in the time of the anneals used (500 minutes). Although the curves appear to level off, the T_c values are likely to continue rising slowly over a period of days (based on experience with other glasses, e.g. $\text{Fe}_{80}\text{B}_{20}$ [19]). Thus on low temperature annealing, far from "equilibrium", the kinetics of relaxation seem to be particularly dependent on the quench rate. It is of interest that now the 16.0 μm and 25.8 μm ribbons behave very differently, the thicker ribbon relaxing more slowly as would normally be expected.

That the curves of T_c vs. time can cross (as in Figure 8) is a manifestation of the "memory" effect in metallic glasses [26]. Two ribbons, though they may attain the same value of T_c during annealing, evidently do not have the same structure, because they do not have identical relaxation behaviour thereafter. The T_c value is not sufficient to describe the contribution of thermal history to the structure of the glass.

3.4 Discussion

The annealing behaviour at 633 K (Figure 7) indicates that all the glasses tend toward the same "equilibrium". If the saturation of the T_c changes indicates true internal equilibrium then this result is expected since the glasses came from the same liquid and should attain the equilibrium liquid structure on annealing. Thus annealing should help to reduce the variability and irreproducibility of properties in

as-quenched samples - something which has often been found to be true. In future work it would be interesting to compare melt-quenched glasses with, e.g., sputtered glasses of the same composition. The latter materials might relax to a different internal equilibrium on annealing, since they do not inherit any short range order from the liquid.

In the Introduction the question was posed: will a fast-quenched glass or a slow-quenched glass be the first to attain a given degree of relaxation on annealing? The fast-quenched glass will relax faster, but it has further to go. The results presented in Figures 7 and 8 show that either answer is possible. At higher annealing temperatures the slow-quenched glass will attain a given state (or rather a given value of a property, in this case T_c) sooner. At lower temperatures, however, the relaxation rate appears to be very sensitive to the quench rate, and a fast-quenched glass may attain a given property value before a slow-quenched one. Since diffusion [27] and viscosity [28] measurements are normally made at low annealing temperatures (to avoid crystallisation) and since these atomic transport properties are particularly sensitive to the degree of relaxation, it is clear that the effect of quench rate in these experiments could be significant.

At 573 K the samples are still far from equilibrium, even after 500 minutes of anneal. The total T_c change corresponding to the attainment of internal equilibrium may be much larger than the differences in initial T_c due to quench rate. The relaxation behaviour is dominated by the faster relaxation of the faster quenched glasses. At 633 K, however, the differences in initial T_c are a significant fraction of the total relaxation range, and the initial differences may prevail, giving rise to a different pattern of behaviour.

This argument may be put in more specific terms. Egami [29] was the first to suggest that there are two mechanisms of relaxation in metallic glasses. His suggestion has been taken up by others: for a discussion see [21]. Here the mechanisms will be called 'short range rearrangement' (SRR), taking place at lower temperatures, and 'long range rearrangement' (LRR) at higher temperatures. Both SRR and LRR contribute to the T_c changes, but the kinetics of the changes are determined primarily by the degree of relaxation or order due to LRR: more LRR gives a more relaxed structure, with slower kinetics. Thus on low temperature annealing SRR occurs, but no LRR. The relaxation kinetics are controlled by the quenched-in LRR-order. The faster quenched glasses, with less quenched-in LRR-order relax faster and continue to do so well into the anneal (Figure 8). At higher annealing temperatures, however, LRR also can take place. During the anneal this acts to diminish the effect of quench rate. The approach to final equilibrium is, then, similar for all the ribbons (Figure 7).

The idea of two relaxation mechanisms is useful in interpreting the anomalous relaxation of the 16.0 μm ribbon. At 573 K its annealing behaviour suggests that it has the lowest degree of LRR-order, as expected for the thinnest (fastest quenched) ribbon. Its initial value of T_c , however, is close to that of the 25.8 μm ribbon. This could arise from a higher initial degree of SRR-order, compensating for the LRR-order. On annealing at 633 K both relaxation mechanisms operate and the overall behaviour of the 16.0 μm and 25.8 μm ribbons can be nearly identical, despite differing contributions from SRR and LRR. That two ribbons can have the same value of a property (in this case T_c), and yet have differing degrees of order due to SRR and LRR, is another example of the memory

effect, and can be readily explained by their thermal history. During the quench the "freezing" temperature for LRR is higher than for SRR. The behaviour of the 16.0 μm ribbon would seem to indicate, therefore, that its quench rate was normal at the temperature where LRR was frozen out, but that the rate became anomalously low at lower temperatures, quenching in too high a degree of SRR-order. This would be the case, for example, if the ribbon came off the wheel sooner than expected. Obviously, characterising the quench by a single rate is an oversimplification.

4. CONCLUSIONS

Measurements of Curie temperature, T_c , can be used to monitor structural relaxation in $\text{Fe}_{81.5}\text{B}_{14.5}\text{Si}_4$ glass. Faster quenching produces less relaxed glasses, affecting not only the properties of the as-produced materials, but also their behaviour on annealing. Structural relaxation is faster in fast-quenched than in slow-quenched glasses, particularly at low annealing temperatures. All the glasses, however, tend to the same equilibrium on annealing. The results can be interpreted in terms of two relaxation mechanisms.

5. ACKNOWLEDGMENTS

The author is grateful to Drs. H.H. Liebermann and F.E. Luborsky of the General Electric Company for supplying the materials used in this work, and to Professors T. Egami (University of Pennsylvania) and F. Spaepen (Harvard University) for useful discussions. This work was supported by the Office of Naval Research under contract N00014-77-C-0002, and was carried out during the tenure of a NATO Research Fellowship awarded by the Science Research Council (U.K.).

REFERENCES

1. H.H. Liebermann and C.D. Graham, Jr., IEEE Trans. Magn. MAG-12 (1976) 921.
2. H. Hillmann and H.R. Hilzinger, Rapidly Quenched Metals III (ed. B. Cantor), Vol. 1, p. 28. London: Metals Society (1978).
3. J.H. Vincent and H.A. Davies, Proc. Conf. on Solidification Technology, Warwick (1980).
4. R.C. Ruhl, Mater. Sci. & Eng., 1 (1967) 313.
5. J.D. Livingston, Physica Stat. Sol. (a), 56 (1979) 637.
6. H.S. Chen and D.E. Polk, J. Non-Cryst. Sol., 15 (1974) 174.
7. B.G. Lewis and H.A. Davies, The Structure of Non-Crystalline Materials (ed. P.H. Gaskell), p. 89. London: Taylor and Francis (1977).
8. G.C. Chi, H.S. Chen and C.E. Miller, J. Appl. Phys., 49 (1978) 1715.
9. S. Takayama and T. Oi, J. Appl. Phys. 50 (1979) 1595.
10. F.E. Luborsky and J.L. Walter, Mater. Sci. and Eng. 35 (1978) 255.
11. F.E. Luborsky and H.H. Liebermann, J. Appl. Phys. 51 (1980) 796.
12. T. Mizoguchi, S. Hatta, H. Kato, H. Arai, K. Maeda and N. Akutsu, IEEE Trans. Magn., MAG-16 (1980) 1147.
13. L. Novak, L. Potocky, A. Lovas, E. Kisdi-Kuszo and J. Takacs, J. Magn. Magn. Mat. 19 (1980) 149.
14. A. Lovas, C. Hargitai, E. Kisdi-Kuszo, J. Takacs, J. Kiraly and G. Sos, J. Magn. Magn. Mat. 19 (1980) 168.
15. F.E. Luborsky, H.H. Liebermann and J.L. Walter, Proc. Conf. on Metallic Glasses: Science and Technology, Budapest (1980).
16. P. Allia, F.E. Luborsky, R. Sato Turtelli, G.P. Soardo and F. Vinai, IEEE Trans. Magn. Nov. 1981 (to be published).
17. F.E. Luborsky, J.J. Becker and R.O. McCary, IEEE Trans. Magn. MAG-11 (1975) 1644.
18. R.S. Williams and T. Egami, IEEE Trans. Magn. MAG-12 (1976) 927.
19. A.L. Greer, Thermochim. Acta 42 (1980) 193.
20. A.L. Greer, M.R.J. Gibbs, J.A. Leake and J.E. Evetts, J. Non-Cryst. Solids 38 and 39 (1980) 379.

21. A.L. Greer and F. Spaepen, Ann. N.Y. Acad. Sci. (1981) in press.
22. J.C. Swartz, R. Kossowsky, J.J. Haugh and R.F. Krause, J. App. Phys. 52 (1981) 3324.
23. J.C. Swartz, J.J. Haugh, R.F. Krause and R. Kossowsky, J. Appl. Phys. 52 (1981) 1908.
24. J. Durand and M. Yung, "Amorphous Magnetism II". (eds. R.A. Levy and R. Hasegawa), p. 275. Plenum Press, New York (1977).
25. A.L. Greer, Acta Metall. (1981) in press.
26. A.L. Greer and J.A. Leake, J. Non-Cryst. Solids 33 (1979) 291.
27. M. Kijek, M. Ahmadzadeh, B. Cantor and R.W. Cahn, Scr. Metall. 14 (1980) 1337.
28. A.I. Taub and F. Spaepen, Acta Metall. 28 (1980) 1781.
29. T. Egami, Mater. Res. Bull. 13 (1978) 557.

FIGURE CAPTIONS

Figure 1. Effect of heating rate on the Curie temperature measured by DSC.

Temperature lags in the instrument have been accounted for.

Figure 2. The rise in Curie temperature on 15 min. anneals at selected temperatures. Initial values: 633.6 K for the 25.8 μm ribbon; 637.6 K for the 58.2 μm ribbon.

Figure 3: DSC curves obtained on heating samples from a 21.6 μm ribbon of $\text{Fe}_{81.5}\text{B}_{14.5}\text{Si}_4$ glass at 40 K min^{-1} . Pre-annealing can drive the first, exothermic reaction to completion.

Figure 4. Transmission electron micrograph of 21.6 μm ribbon of $\text{Fe}_{81.5}\text{B}_{14.5}\text{Si}_4$ glass pre-annealed at 718 K for 20 minutes. Dendritic α -Fe crystals in an amorphous matrix.

Figure 5. The increase in Curie temperature on annealing a 21.6 μm ribbon of $\text{Fe}_{81.5}\text{B}_{14.5}\text{Si}_4$ glass at 718 K. Primary crystallisation occurs during the anneal.

Figure 6. The initial Curie temperatures of five ribbon thicknesses of $\text{Fe}_{81.5}\text{B}_{14.5}\text{Si}_4$ glass. Each point is the average of six measurements.

Figure 7. The increase in Curie temperature on annealing ribbons of $\text{Fe}_{81.5}\text{B}_{14.5}\text{Si}_4$ glass at 633 K. All samples tend to the same equilibrium. (Each point represents the average of at least two measurements).

Figure 8. The increase in Curie temperature on annealing ribbons of $\text{Fe}_{81.5}\text{B}_{14.5}\text{Si}_4$ glass at 573 K. (Each point represents the average of at least two measurements.)

Figure 1

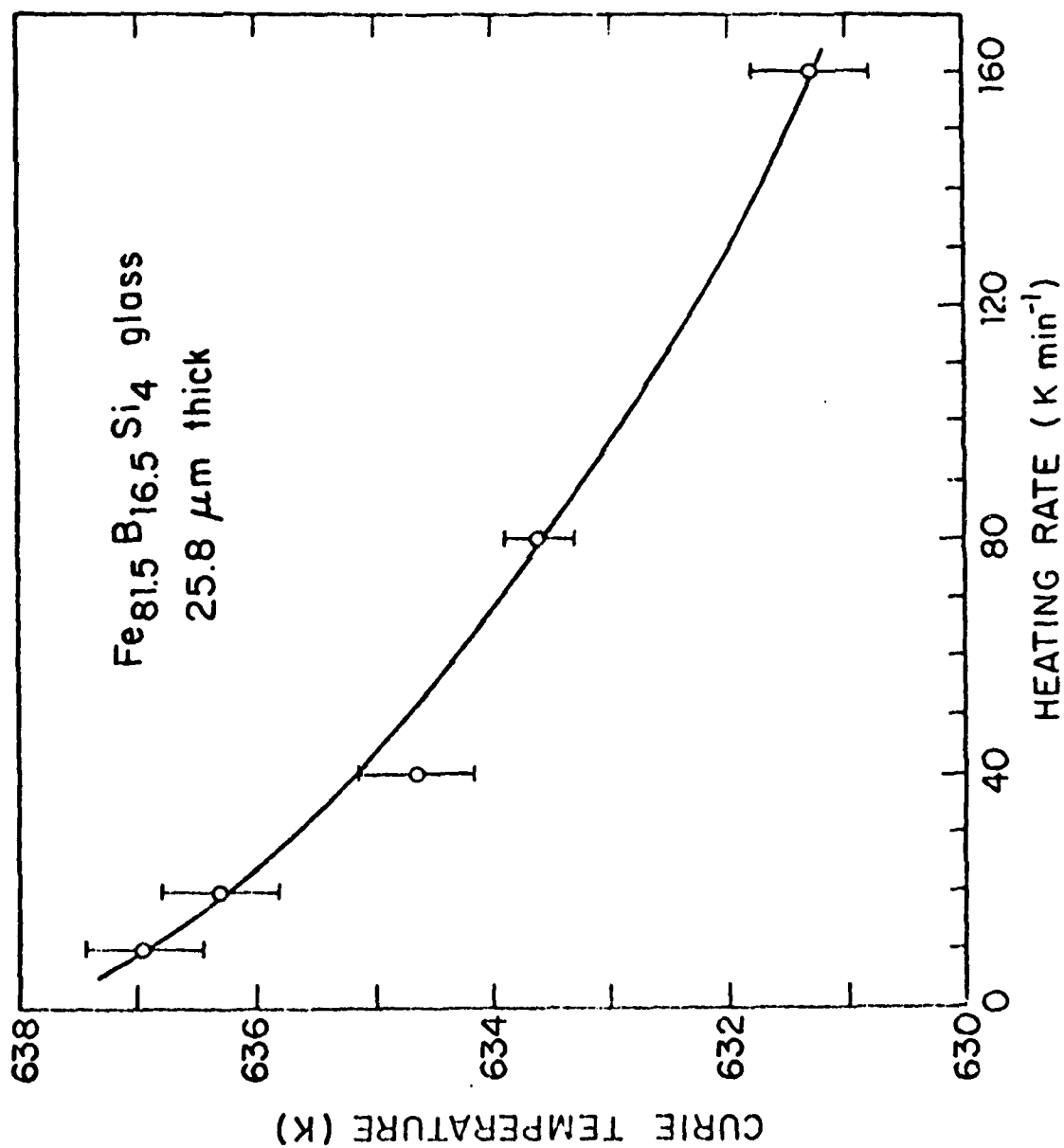


Figure 2

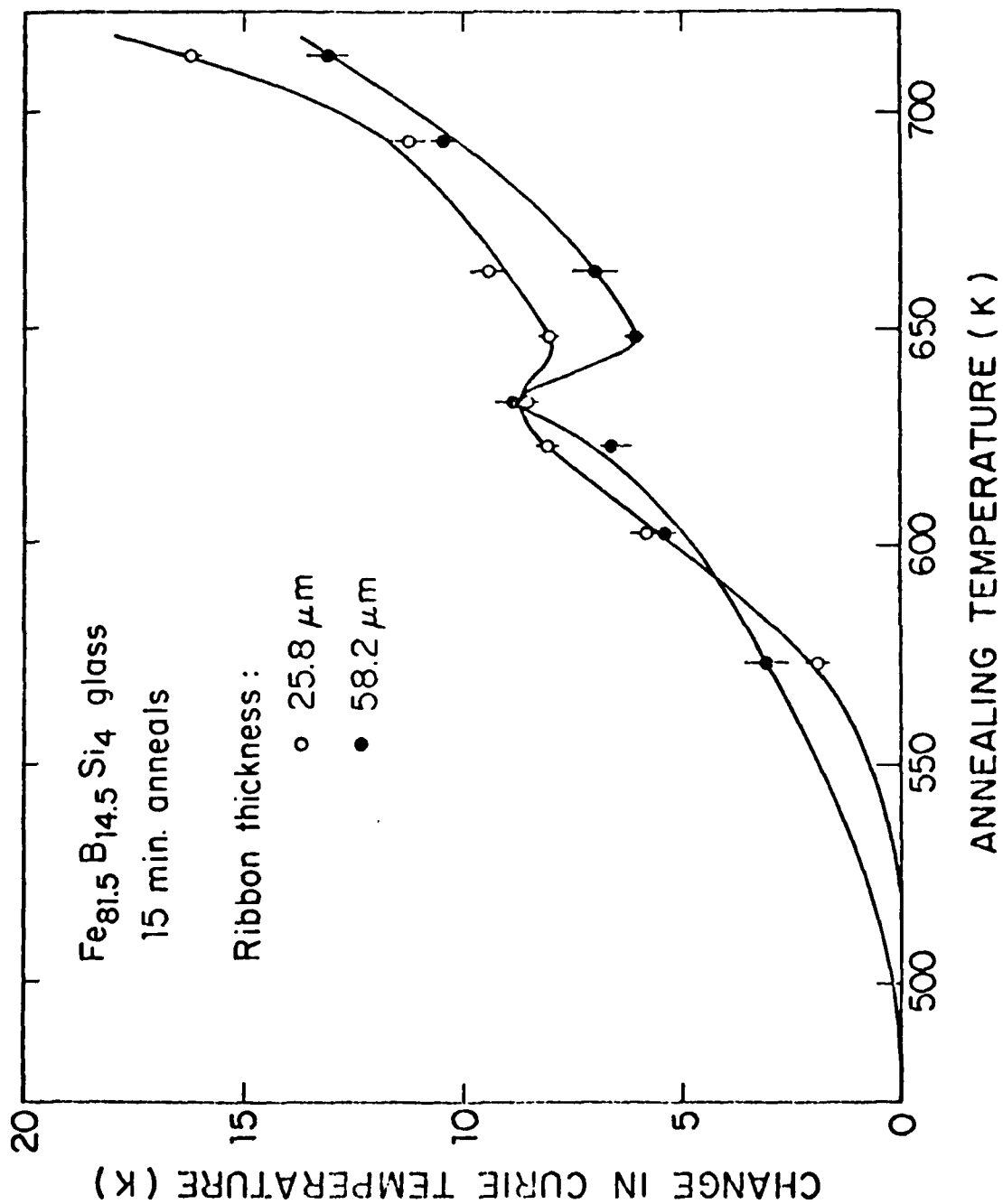


Figure 3.

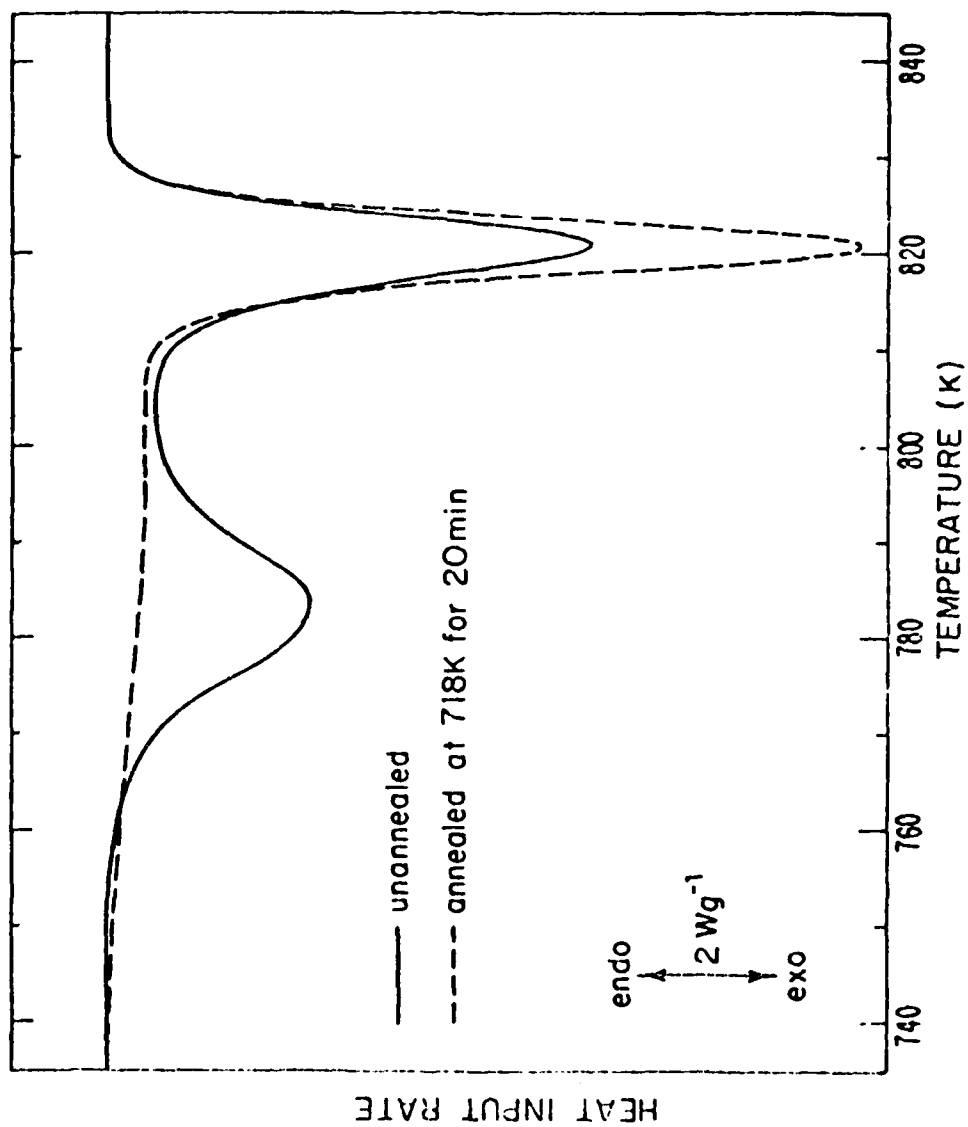


Figure 4.



Figure 5

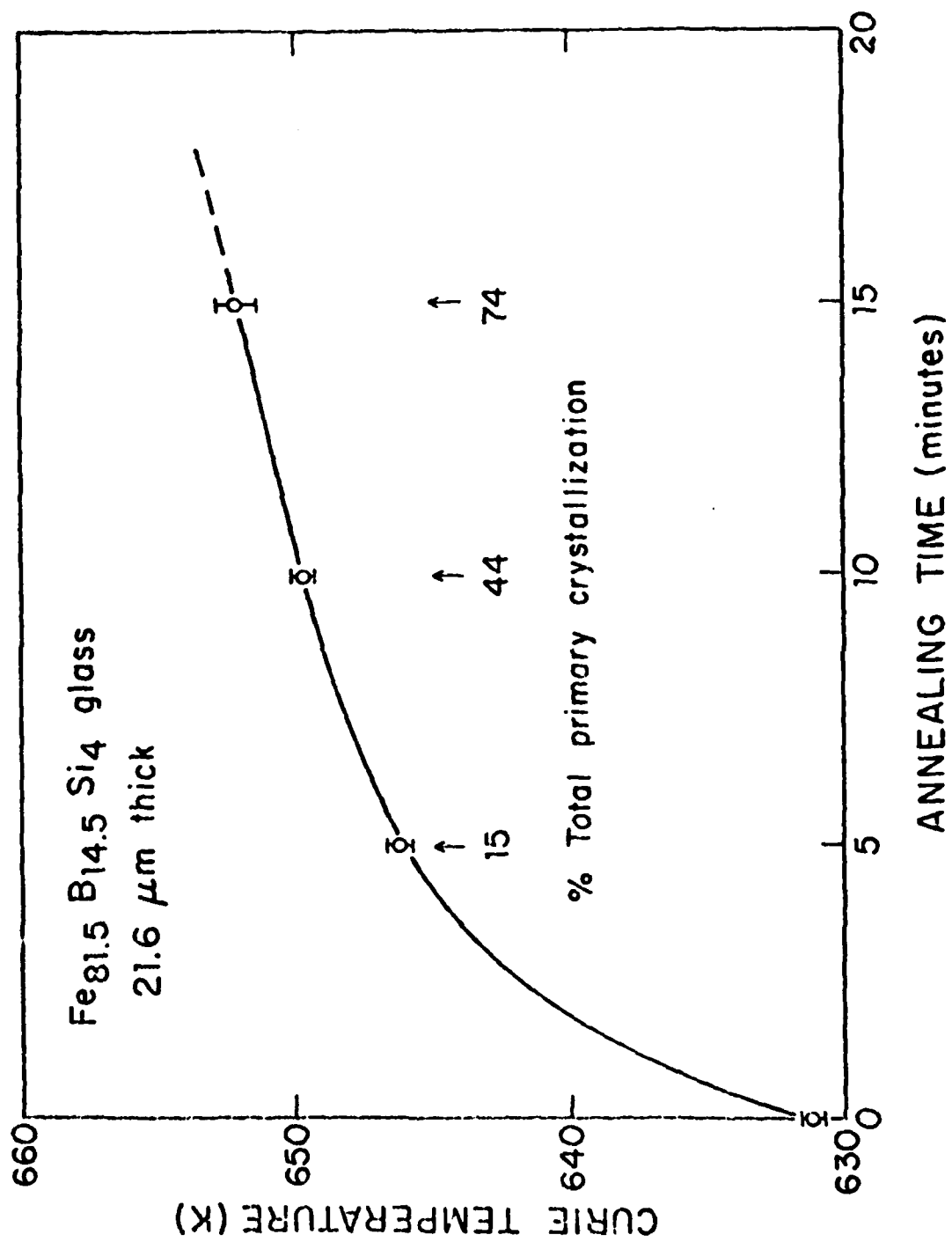


Figure 6

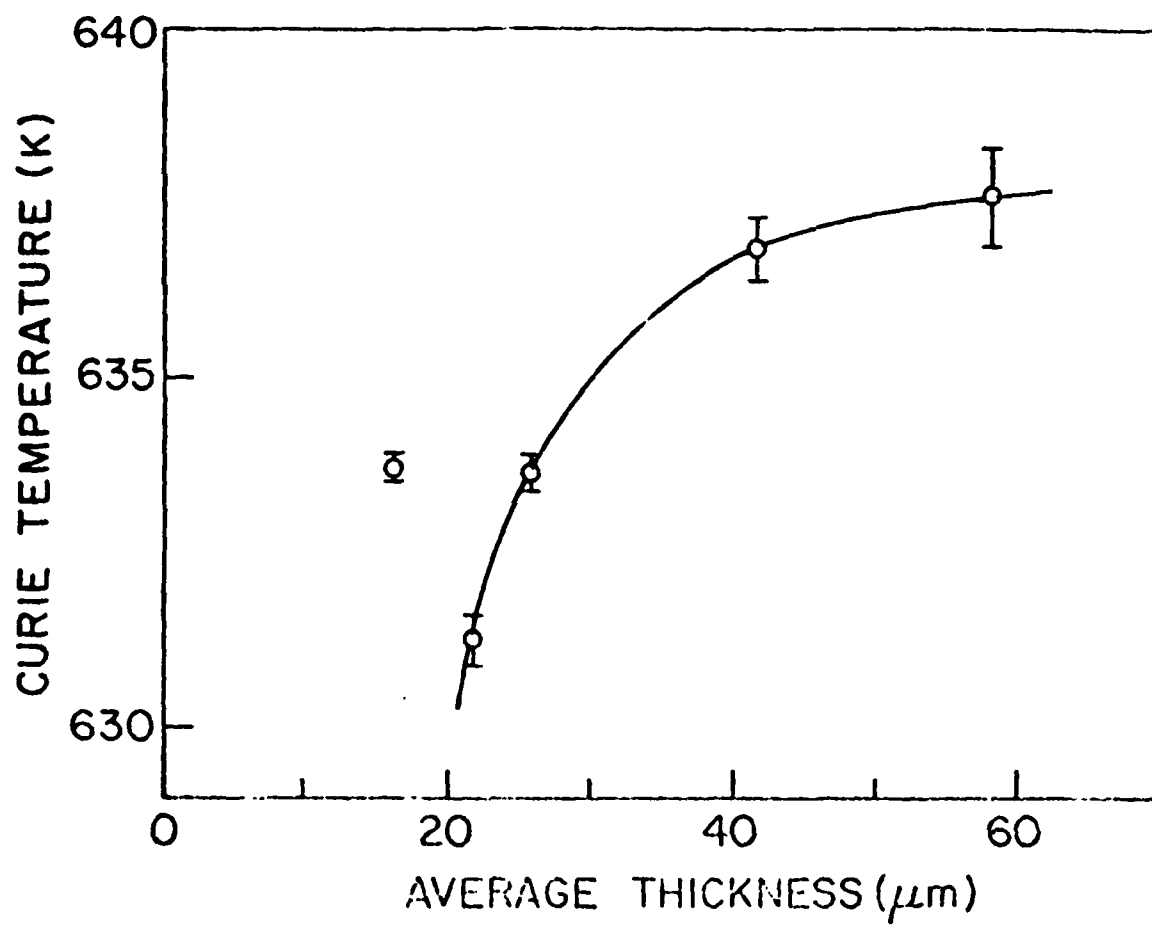


Figure 7

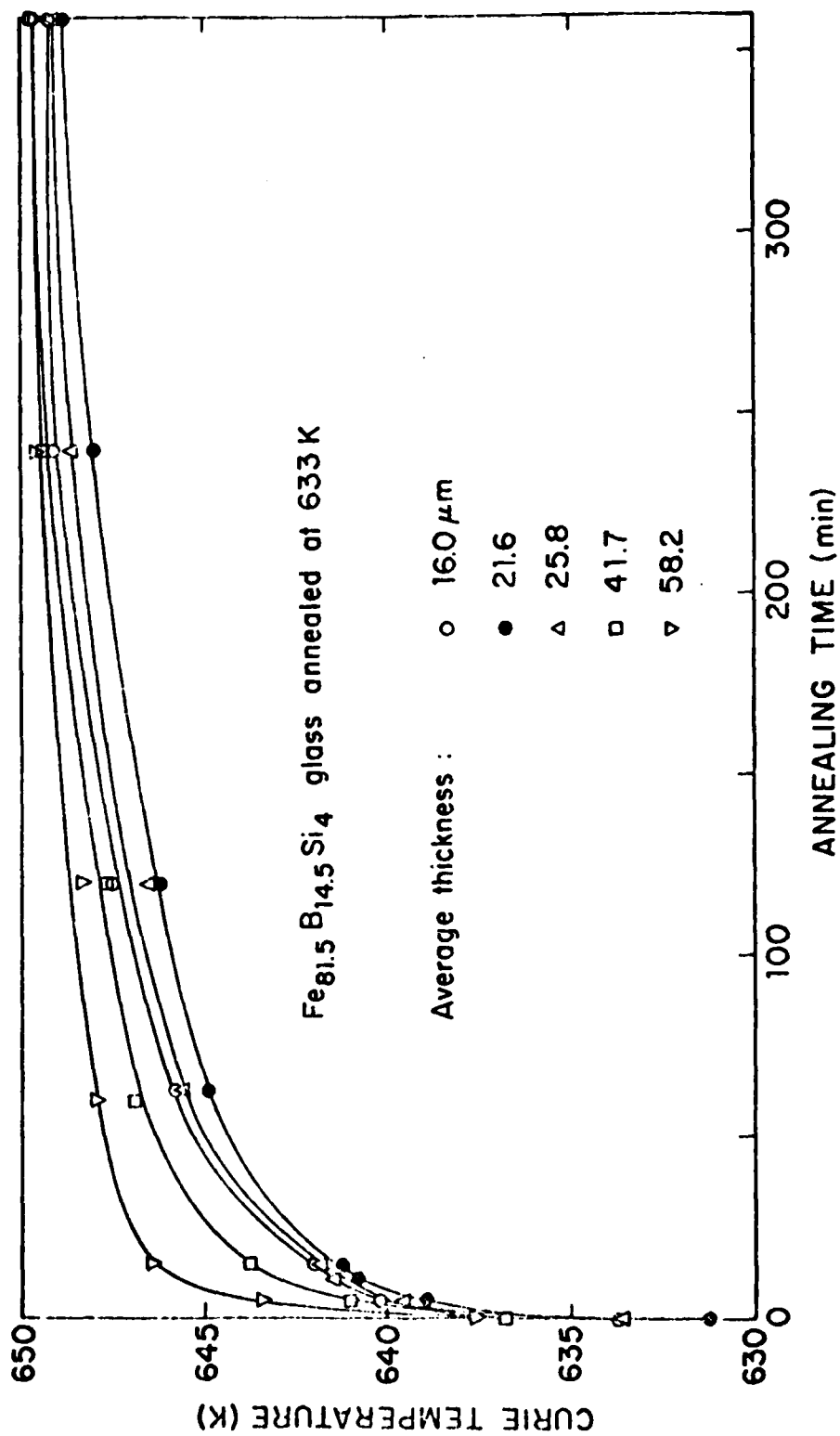
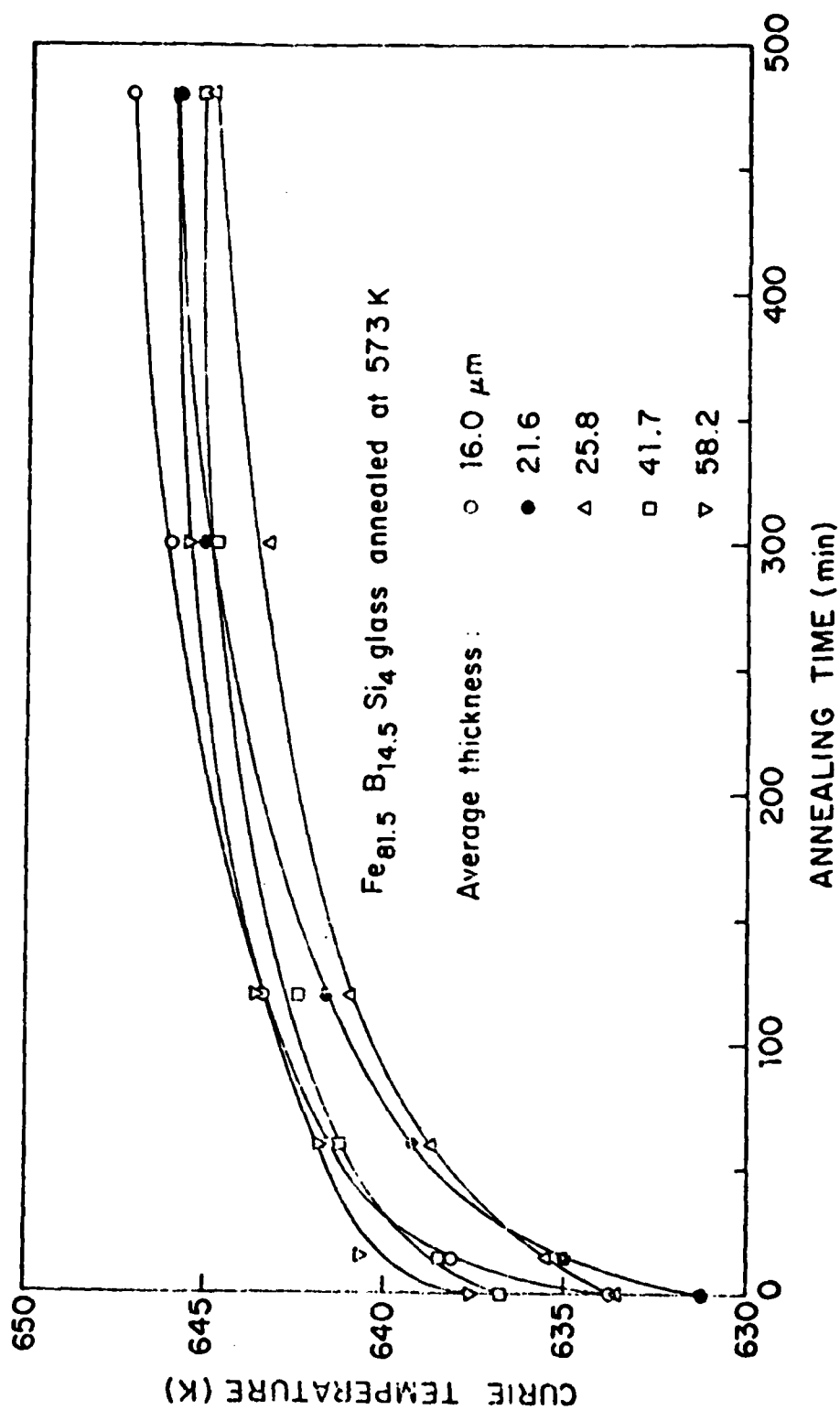


Figure 8



Defense Documentation Center
Camden Station
Alexandria, Virginia 22304 (12)

Office of Naval Research
Department of the Navy
Attn: Code 971 (3)
Code 105 (6)
Code 470

Director
Office of Naval Research
Branch Office
495 Summer Street
Boston, Massachusetts 02210

Director
Office of Naval Research
Branch Office
536 South Clark Street
Chicago, Illinois 60605

Office of Naval Research
San Francisco Area Office
760 Market Street, Room 447
San Francisco, California 94102

Naval Research Laboratory
Washington, D.C. 20390

Attn: Code 6000 (6)
Code 6100
Code 6300
Code 6400
Code 2627

Attn: Mr. F.S. Williams
Naval Air Development Center
Code 101
Warminster, Pennsylvania 18974

Naval Air Propulsion Test Center
Trenton, New Jersey 08628
Attn: Library

Naval Weapons Laboratory
 Dahlgren, Virginia 22448
Attn: Research Division

Naval Construction Battalion
Civil Engineering Laboratory
Port Hueneme, California 93043
Attn: Materials Division

Naval Electronics Laboratory Center
San Diego, California 92152
Attn: Electronic Materials Sciences Div.

Naval Missile Center
Materials Consultants
Code 3312-1
Point Mugu, California 93041

Commanding Officer
Naval Ordnance Laboratory
White Oak
Silver Spring, Maryland 20910
Attn: Library

Naval Ship R and D Center
Materials Department
Annapolis, Maryland 21402

Naval Undersea Center
San Diego, California 92132
Attn: Library

Naval Underwater System Center
Newport, Rhode Island 02840
Attn: Library

Naval Weapons Center
Chico Lake, California 93555
Attn: Library

Naval Postgraduate School
Monterey, California 93940
Attn: Materials Sciences Dept.

Naval Air Systems Command
Washington, D.C. 20360
Attn: Code 52031
Code 52032
Code 320

Naval Sea System Command
Washington, D.C. 20362
Attn: Code 035

Naval Facilities
Engineering Command
Alexandria, Virginia 22331
Attn: Code 03

Scientific Advisor
Commandant of the Marine Corps
Washington, D.C. 20380
Attn: Code A5

Naval Ship Engineering Center
Department of the Navy
Washington, D.C. 20360
Attn: Director, Materials Sciences

Army Research Office
Box CM, Duke Station
Durham, North Carolina 27706
Attn: Metallurgy and Ceramics Div.

Army Materials and Mechanics
Research Center
Watertown, Massachusetts 02172
Attn: Res. Programs Office (AMMR-P)

Commanding General
Department of the Army
Ft. Belvoir Arsenal
Philadelphia, Pennsylvania 19137
Attn: OKDBA-1320

Office of Scientific Research
Department of the Air Force
Washington, D.C. 20331
Attn: Solid State Div. (SRPS)

Aerospace Research Labs
Wright-Patterson AFB
Building 450
Dayton, Ohio 45433

Air Force Materials Lab (LA)
Wright-Patterson AFB
Dayton, Ohio 45433

NASA Headquarters
Washington, D.C. 20546
Attn: Code RRM

NASA
Lewis Research Center
21000 Brexton Road
Cleveland, Ohio 44135

National Bureau of Standards
Washington, D.C. 20234
Attn: Metallurgy Division
Inorganic Materials Division (6)

Atomic Energy Commission
Washington, D.C. 20545
Attn: Metals and Materials Branch

Defense Metals and Ceramics
Information Center
Battelle Memorial Institute
505 King Avenue
Columbus, Ohio 43201

Director
Ordnance Research Laboratory
P.O. Box 30
State College, Pennsylvania 16801

Director Applied Physics Lab
University of Washington
16113 Northeast Fourth Street
Seattle, Washington 98105

Metals and Ceramics Division
Oak Ridge National Laboratory
P.O. Box 8
Oak Ridge, Tennessee 37830

Los Alamos Scientific Lab.
P.O. Box 1663
Los Alamos, New Mexico 87544
Attn: Report Library

Argonne National Laboratory
Metallurgy Division
P.O. Box 229
Lemont, Illinois 60439

Brookhaven National Laboratory
Technical Information Division
Upton, Long Island
New York 11973

Attn: Research Library

Library
Building 50, Room 134
Lawrence Radiation Laboratory
Berkeley, California

Professor G.S. Ansell
Rensselaer Polytechnic Institute
Dept. of Metallurgical Engineering
Troy, New York 12181

Professor H.K. Burnbaum
University of Illinois
Department of Metallurgy
Urbana, Illinois 61801

Dr. E.M. Brennan
United Aircraft Corporation
United Aircraft Research Lab
East Hartford, Connecticut 06108

Professor H.D. Brady
University of Pittsburgh
School of Engineering
Pittsburgh, Pennsylvania 15213

Professor J.B. Cohen
Northwestern University
Dept. of Material Sciences
Evanston, Illinois 60201

Professor M. Cohen
Massachusetts Institute of Technology
Department of Metallurgy
Cambridge, Massachusetts 02139

Professor B.C. Croesen
Massachusetts Institute of Technology
Department of Chemistry
Boston, Massachusetts 02115

Dr. C.T. Hahn
Battelle Memorial Institute
Department of Metallurgy
515 King Avenue
Columbus, Ohio 43201

Professor R.W. Hechel
Case Western Reserve University
Schenley Park
Pittsburgh, Pennsylvania 15213

Dr. David C. Howden
Battelle Memorial Institute
Columbus Laboratories
505 King Avenue
Columbus, Ohio 43201

Professor C.F. Jachow
Ohio State University
Dept. of Welding Engineering
190 West 18th Avenue
Columbus, Ohio 43210

Professor G. Judd
Rensselaer Polytechnic Institute
Dept. of Materials Engineering
Troy, New York 12181

Dr. C.S. Kortovich
TRW, Inc.
2355 Euclid Avenue
Cleveland, Ohio 44117

Professor D.A. Koss
Michigan Technological University
College of Engineering
Houghton, Michigan 49931

Professor A. Lawley
Drexel University
Dept. of Metallurgical Engineering
Philadelphia, Pennsylvania 19104

Dr. W. Mangin
Polytechnic Institute of New York
331 Jay Street
Brooklyn, New York 11201

Professor K. Masabuchi
Massachusetts Institute of Technology
Department of Ocean Engineering
Cambridge, Massachusetts 02139

Dr. G.H. Meyer
University of Pittsburgh
Dept. of Metallurgical and Materials
Engineering
Pittsburgh, Pennsylvania 15213

Professor J.W. Morris, Jr.
University of California
College of Engineering
Berkeley, California 94720

Professor K. Ono
University of California
Materials Department
Los Angeles, California 90024

Professor W.F. Savage
Rensselaer Polytechnic Institute
School of Engineering
Troy, New York 12181

Dr. C. Shaw
Rockwell International Corp.
P.O. Box 1003
1049 Camino Dos Rios
Thousand Oaks, California 91360

Professor O.D. Sherby
Stanford University
Materials Sciences Dept.
Stanford, California 94305

Professor J. Shyne
Stanford University
Materials Sciences Department
Stanford, California 94305

Dr. W.A. Spitzig
U.S. Steel Corporation
Research Laboratory
Monroeville, Pennsylvania 15146

Dr. E.A. Starke, Jr.
Georgia Institute of Technology
School of Chemical Engineering
Atlanta, Georgia 30332

Professor N.S. Stoloff
Rensselaer Polytechnic Institute
School of Engineering
Troy, New York 12181

Dr. E.R. Thompson
United Aircraft Research Lab
400 Main Street
East Hartford, Connecticut 06108

Professor David Taraball
Harvard University
Division of Engineering and Applied
Physics
Cambridge, Massachusetts 02139

Dr. F.W. Wang
Naval Ordnance Laboratory
Physics Laboratory
White Oak
Silver Spring, Maryland 20910

Dr. J.C. Williams
Rockwell International
Science Center
P.O. Box 1003
Thousand Oaks, California 91360

Professor M.C.F. Wilsdorf
University of Virginia
Department of Materials Science
Charlottesville, Virginia 22903

Dr. M.A. Wright
University of Tennessee
Space Institute
Dept. of Metallurgical Engineering
Tullahoma, Tennessee 37388

DATE
FILMED
8